ELSEVIER

Polymer 42 (2001) 7653–7661

polymer

www.elsevier.nl/locate/polymer

Characterization of melt-polymerized polycarbonate: preparative fractionation, branching distribution and simulation

A.C. Hagenaars[a], J.-J. Pesce[b], Ch. Bailly[a,*], B.A. Wolf [c]

[a]*Laboratoire des Hauts Polymères, Université Catholique de Louvain, 1348 Louvain-la-Neuve, Belgium*
[b]*30 Rue Romain Rolland, 71230 Saint-Vallier, France*
[c]*Institut für Physikalische Chemie der Universität Mainz, Jakob-Welder Weg 13, 55099 Mainz, Germany*

Received 7 February 2001; accepted 26 March 2001

Abstract

Melt-polymerized bisphenol-A polycarbonate materials characterized by a low degree of branching were fractionated according to molecular weight by the continuous polymer fractionation (CPF) method. The distribution of two types of end-groups and in-chain salicylate moieties arising from thermal rearrangement reactions were assessed across the molecular weight distribution by analysis of the fractions. Experimentally determined branching densities of the fractions agreed well with a molecular simulation based on a random sampling polycondensation model. Both simulation and experiments showed that the branching density increases with molecular weight in the experimentally accessible range. © 2001 Elsevier Science Ltd. All rights reserved.

Keywords: Polycarbonate; Bisphenol-A; Melt polymerization

1. Introduction

Bisphenol-A based polycarbonate (BPA-PC) is an important thermoplastic engineering material with unique properties including high transparency, high impact strength and dimensional stability. Two commercial processes are currently used to produce BPA-PC: the phosgenation process where BPA is reacted interfacially with phosgene in a water–organic solvent system and the melt transesterification process where BPA is reacted with diphenyl carbonate (DPC) at elevated temperatures and reduced pressure [1]. Important advantages of the melt process are the absence of solvents and phosgene resulting in a polycarbonate material with an extremely low residual contaminant level. In contrast, the molecular weight (MW) that can be reached is limited and complicated equipment is needed to control high temperatures, low pressures and high polymer viscosities. Combinations of excessive residence time and high temperatures in the reactor can lead to side reactions resulting in discoloration and branching [2,3].

The most widely accepted mechanism for thermal rearrangements of PC in the melt is a base-catalyzed Kolbe–Schmitt reaction [2]. The following structures have been shown to result from this mechanism: phenyl salicylate (PhSAL, structure I), phenyl salicylate phenyl carbonate (PhSALPhC, structure II) and phenyl-*o*-phenoxy benzoate (Ph-*o*-PhxBz, structure III) [2,4,5]. The corresponding PC structures are shown in Fig. 1.

Characterization of branched PC materials is gaining renewed attention as evidenced by some very recent publications [3,6]. While the structure of melt-polymerized PC branching units is reasonably well understood, their distribution across the MW distribution has never been studied in detail. In an early paper, Bartosiewicz et al. [7] investigated branching in commercial BPA-PC materials where the presence of phenyl-*o*-phenoxy benzoate branching units (structure III in this paper) was only hypothesized. Some evidence for random distribution of branching units was found. It is well-known that branching can have a significant influence on the rheological [8] and mechanical [9] properties of polymers and a detailed understanding of the branching distribution is therefore of major importance.

The objective of this paper is to study the distribution of modified units (structures I to III) across the MW distribution of two melt-polymerized BPA-PC samples. The experimental study involves fractionation by MW followed by analytical characterization of the fractions. Besides structure characterization, a major goal of the fractionation experiments was to obtain large size fractions to be used for further rheological and mechanical testing. This aspect

* Corresponding author.
E-mail address: bailly@poly.ucl.ac.be (C. Bailly).

PII: S0032-3861(01)00250-6

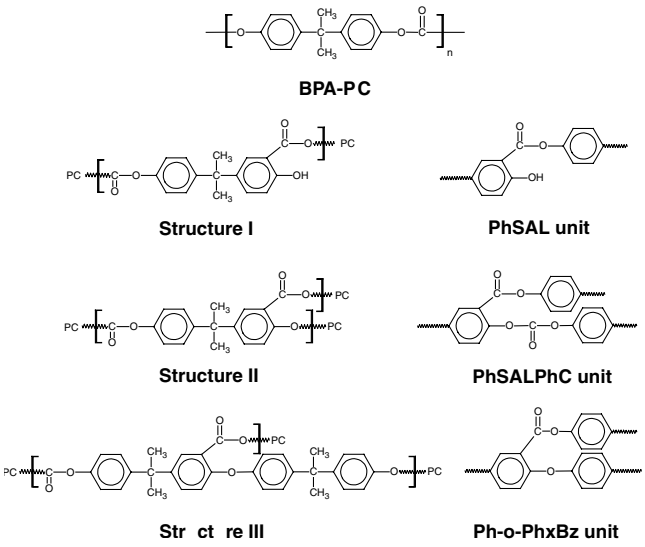

Fig. 1. Polycarbonate melt rearrangement structures.

will be covered in subsequent publications. Experimental results have also been validated by a simulation model.

1.1. Random branching

Branching species in polymer materials can be distributed randomly or non-randomly. We define random branching in the usual way, i.e. the probability that any monomeric unit carries a branching point is independent of the status of other units in the same chain [10]. In fact, the random incorporation of branching species in a polymer chain in the ideal case is a mere statistical process. Randomly branched polymers will be called homogeneous if the branching probability is the same irrespective of the sampled chain. Polymerization reactions where the residence time in a reactor is different for individual molecules, for instance, may lead to heterogeneous branching. An example is the class of branched polymers that are made through free-radical polymerization with chain transfer when distribution of residence times in the reactor is large [11]. This can lead to the so-called intermolecular heterogeneity.

The concentration of branching species in a polymer chain is expressed through the branching density, ρ, which is defined as

$$\rho = \frac{\text{number of branching units}}{\text{total number of units bound}} \tag{1}$$

For branched polymers obtained by random grafting of a most probable distribution of linear chains, Tobita [11,12] has recently shown that the branching density as a function of degree of polymerization, ρ_r, initially increases with MW and eventually reaches a fixed value for high MW species according to the following relation:

$$\rho_r = \frac{\sqrt{\rho/u}I_2(2r\sqrt{\rho/u})}{I_1(2r\sqrt{\rho/u})} \tag{2}$$

where ρ is the average branching density, r the degree of polymerization, u the number average chain length of the primary distribution of linear chains and I_1 and I_2 the modified Bessel functions of the first and second order, respectively. Well-known theories describing the MW distribution and branching density of branched step-growth polymers apply formally only to cases where all monomers are present from the start of the reaction. In the case of melt-polymerized PC, however, branching species are being formed as a result of thermal rearrangement reactions potentially occurring during the later stages of the polymerization process, and the existing theories should be applied with caution.

An elegant way to treat complex cases of non-linear polymerizations is by simulation. A model can be designed based on all characteristics of a specific polymerization process. Simulation models based on random sampling can deliver detailed information on the MW distribution and branching architecture of polymers. Their usefulness and correctness should, however, always be validated by experimental methods.

1.2. Continuous polymer fractionation of branched BPA-PC

A practical method to determine the branching density (and other modifications) across a MW distribution is by fractionation [13]. This is a widely applied technique to divide polymeric materials into narrowly dispersed fractions based on differences in MW, crystallinity properties or chemical composition and valuable information can be derived on the distribution of end-groups, functional groups, branching units and co-monomers across the entire MW range [14].

Polycarbonate can be fractionated by most common fractionation methods including precipitation fractionation procedures [15–18], column fractionation techniques [19,20] and chromatographic methods [21]. All methods in principle are capable of delivering any desired number of narrowly dispersed fractions. The difficulty lies in obtaining fractions of preparative (multi-gram) size that can be used for further research. Large-scale fractionation processes are time consuming and often require significant volumes of solvents.

The continuous polymer fractionation (CPF) technique has been especially developed to produce preparative size fractions in a short time frame with the use of limited volumes of solvents [22,23]. CPF has been proven successful for linear polycarbonates [24,25] but has never been employed for branched polycarbonate materials. In CPF, fractions of increasing MWs are removed from a concentrated polymer solution ('feed') by a proceeding liquid–liquid extraction in a counter-current process with a single solvent or solvent/non-solvent mixture ('extracting agent'). A solvent/non-solvent mixture is preferred as it facilitates tailoring of the process. The feed and the extracting agent are introduced into the extraction device (e.g. a column) as

homogeneous phases. For properly chosen fluxes, these liquids do not mix homogeneously as they meet but form two phases of different density, which are transported against each other in the terrestrial gravitational field. By exchange of matter over the phase boundaries, the polymer-rich gel phase and the polymer-lean sol phase are gradually being formed. In this process, the lower MW material is extracted by the extracting agent and forms the sol fraction while the higher MW material forms the gel fraction. The (normally less dense) sol fraction leaves the column at its top and the polymer it contains is often isolated for direct use while the gel phase, collected at its bottom, may frequently be directly employed for a second fractionation step. The feed is introduced at a position close to the middle of the column thus preventing a direct contact with the sol phase in which inevitably some high MW material would dissolve resulting in reduced fractionation efficiency. Usually, the two parts of the column above and below the feed introduction position are kept at different temperatures in a way that less soluble material fluxes back before the sol fraction is collected. The fractionation process can be optimized by changing either the solvent/non-solvent composition, the temperature or the flow rate of feed and extraction agent. Preliminary experiments for CPF include determination of the miscibility gap of the polymer–solvent mixture. This is accomplished by measuring cloud-points in the concentration range of interest for CPF. Tie-lines connecting the conjugated sol and gel phases can be found by demixing ternary systems with overall composition inside the miscibility gap and subsequently analyzing the phase compositions. Also, the so-called working point has to be defined as well as the flow rates of the feed and extracting agent.

Requirements for a successful fractionation are the existence of a good solvent/non-solvent mixture and the possibility to realize liquid–liquid phase separation, a large enough difference in density between the coexisting phases and a controllable viscosity of the system.

It is well known that branching alters the solubility of polymers and fractionation based on phase equilibria will therefore not exclusively take place with respect to MW but inevitably also to some extent according to the branching architecture, where the latter contribution depends on the concentration of branching units in the material. In most cases, fractionation may be at least considered semi-quantitatively useful [13].

It will become clear that the PC samples investigated here were fractionated predominantly according to MW.

2. Experimental

2.1. Samples

Two lab-synthesized polycarbonate samples, PC1 and PC2, were obtained by a melt-transesterification process from BPA and DPC according to literature-described procedures [26,27].

2.2. Continuous polymer fractionation

2.2.1. Equipment

CPF experiments were carried out with a fractionation device combining two glass columns with independent thermostatting control. The lower column is designated as 'column' (length = 1.80 m, diameter = 5 cm); the upper column is designated as 'condenser' (length = 0.60 m, diameter = 5 cm). Both the column and condenser are completely filled with a mixture of glass beads with diameters of 8 mm (50%) and 10 mm (50%). The feed inlet is positioned between the column and the condenser at approximately three-fourths of the total height of the system. The extracting agent inlet is positioned at the bottom of the column. Two piston pumps are used for regulation of feed and extracting agent fluxes. Glass reservoirs are used for supply of feed and extracting agent. CPF equipment is shown in Fig. 2.

2.2.2. Solvents

Methylene chloride: Roth, >99%, synthesis grade.

Diethylene glycol: Acros, 99%.

2.2.3. Determination of cloud-point curves

To construct the phase diagram of the polymer, solvent (methylene chloride) and non-solvent (diethylene glycol), cloud-point curves were recorded at room temperature by titrating polymer solutions with concentrations varying between 4 and 24 w/v% with non-solvent until visible turbidity.

2.2.4. Determination of tie-lines by demixing experiments

Information on the demixing behavior of the polymer/solvent/non-solvent system was obtained by determining tie-lines connecting the conjugated phases. Compositions

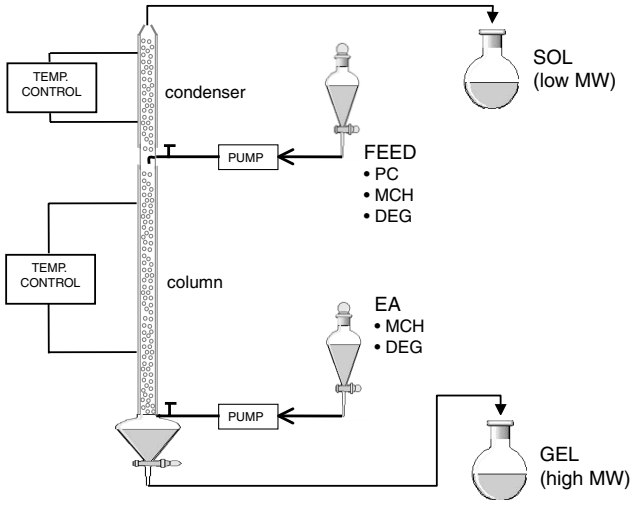

Fig. 2. Experimental CPF set-up.

within the miscibility gap of the phase diagram (at least at a distance of 1 wt% from the cloud-point curve) were selected and prepared in closed vials. The samples were heated on a heating plate at 60°C for several minutes until a clear, homogeneous solution was obtained. The samples were allowed to cool down to room temperature and equilibrate overnight upon which the two-phase system was re-established. Both sol (upper) and gel (lower) phases were collected with a syringe and compositions were measured by means of proton-NMR. Tie lines were obtained by connecting sol and gel compositions in the ternary phase diagram.

2.2.5. Working line

The working line connects feed and EA compositions. The working point, which is situated on the working line, was determined graphically in the ternary phase diagram by means of known ratio of the fluxes of feed and extracting agent.

2.2.6. Isolation of fractions

From collected feed and sol fractions, dichloromethane was removed by evaporation at 40°C under reduced pressure by means of a rotation evaporator. The precipitated polymer was separated from the remaining non-solvent by filtration over a Buchner funnel and extracted several times with excess methanol to remove the last traces of diethylene glycol. By this procedure, the diethylene glycol content in the fractions is lower than 20 ppm as determined by proton-NMR. The applied isolation procedure has no influence on the chemical structure or MW of the fractions as confirmed by NMR and SEC.

2.3. Size exclusion chromatography

2.3.1. SEC-UV

Measurements were run on a system consisting of a Waters model 590 pump, a Waters WISP 717 plus autosampler device and a Waters 486 tuneable UV absorbance detector. Polycarbonate samples in methylene chloride (0.1 w/v%) containing 0.025% toluene as flow marker were filtered through 0.45μ Schleicher and Schuell Greenband filters and injected on the SEC system at an injection volume of 50 μl. Two PL-gel 5μ 300 mm × 7.5 mm columns, 10^3 and 10^5 Å, were used in series with methylene chloride as mobile phase. Flow rate was 1.0 ml/min. The eluted polymer was detected at 254 nm. Total run time was 24 min. Calibration was performed against a series of polycarbonate standards with known absolute MWs. Data manipulation: Perkin–Elmer Nelson Turbochrom 4 software.

2.3.2. SEC-LS/IV/RI

Absolute MWs were measured on a Hewlett Packard 1100 SEC system coupled to a Viscotek 300TDA Triple detector combining a right angle laser light scattering detector (RALLS), a four-capillary differential viscometer and a differential refractometer. Sample preparation, column configuration, mobile phase and flow rate as for SEC-UV. Injection volume was 100 μl. Data manipulation: Viscotek TriSEC software.

2.4. NMR

Proton-NMR measurements were run on a Bruker Avance 400 spectrometer using a 5 mm i.d. Quadro Nuclei Probe. A pulse width of 90° (10 μs), relaxation time of 4 s and acquisition time of 2.6 s were employed. Automatic digital quadrature detection was applied. Data manipulation: Bruker XwinNMR software.

Sol and gel phases obtained from demixing experiments for determination of tie-lines were prepared at a concentration of 5 w/v% in d-chloroform. 128 free induction decays (FIDs) were collected for compositional analysis of the phases. CPF fractions were dissolved in d-chloroform at a concentration of 5–10 w/v%. 1024 FIDs were collected for analysis of the fractions. PhSAL structures were quantified by integrating the absorbance at 8.01 ppm after deconvolution from a neighboring peak against the total absorbance of aromatic protons in the region between 6.5 and 7.6 ppm.

PhSALPhC branching structures were similarly quantified by using the absorbance at 8.14 ppm. Both PhSAL and PhSALPhC absorbances exhibit a 3J doublet-splitting pattern resulting from long-range proton–proton coupling effects.

The hydroxyl end-group concentration of the fractions was determined by integrating the absorbance at 6.62 ppm against the total absorbance of aromatic protons.

2.5. Simulation model

A random simulation model has been written in Visual Basic in order to determine the statistical chain configuration for each MW species of a polymeric melt-polymerized BPA-PC system. In each simulation, BPA, DPC and branching units (structure II) were linked randomly. A total of 10^6 BPA monomers were used in each simulation experiment. The number of DPC monomers follows then from a calculation of the stoichiometry of the system. It is related to the number average MW and the endcap level (i.e. the ratio between phenyl carbonate and bisphenol-A end-groups) of the polymer to be simulated, both determined experimentally from SEC and NMR results. The number of branching units used in the model was equal to the experimentally determined concentration of these units. The program output includes information on the MW distribution, branching density distribution and endcap level of the simulated polymer.

3. Results and discussion

3.1. Fractionation of samples

For the fractionation of samples PC1 and PC2 by CPF, a

solvent/non-solvent/polymer system was used consisting of methylene chloride (MCH), diethylene glycol (DEG) and the polymer (PC). It was shown in previous studies [24,25] that when using MCH as solvent and DEG as non-solvent, specific problems related with the fractionation of PC such as degradation and crystallization are prevented. Fractionation was carried out in a column filled with glass beads. The glass beads decrease the interstitial volume and consequently the capacity of the column but significantly increase the efficiency of the fractionation by delaying the descent of the gel particles in the column and, hence, prolong the effective fractionation period. Feed and EA compositions are chosen in a way that their connecting working line lies approximately parallel with the experimental tie-lines. Prior to execution of the CPF runs, cloud-point curves were recorded for the starting polymers to determine the miscibility gap in the concentration range of the fractionation. For PC1, the polycarbonate fraction isolated from the gel phase of the first CPF run was used for the second fractionation experiment. For this purpose, a second cloud-point curve was recorded. In case of PC2, the gel phase obtained after the first fractionation run was used as such for the second fractionation experiment without isolation of the polymer.

The phase diagram for PC1 comprising of the cloud-point curve, tie-lines and working line is shown in Fig. 3. Data points representing the compositions of the initial polymer/solvent/non-solvent mixture and sol and gel phases of the experimentally determined tie-lines are not positioned exactly on a straight line. This is mainly due to evaporation of the highly volatile methylene chloride during the applied measurement procedure. The phase diagram for PC2 looks very similar and is not reproduced here.

Samples PC1 and PC2 were fractionated into three and four fractions, respectively. Fraction nr. 3 of PC2 was isolated from the column content, which was collected directly after termination of the second fractionation run.

The choice for a limited number of large size fractions goes to some extent at the cost of narrowness of the dispersion of the fractions. Narrower dispersions could easily be obtained by increasing the number of fractionation steps and scaling down of the equipment (e.g. the use of glass beads with smaller diameters) [24]. This would consequently prolong the fractionation time. With the used experimental CPF set-up, PCs can be fractionated at a rate of roughly 10–15 g/h. Experimental CPF parameters for the fractionation of polycarbonate samples PC1 and PC2 are given in Table 1.

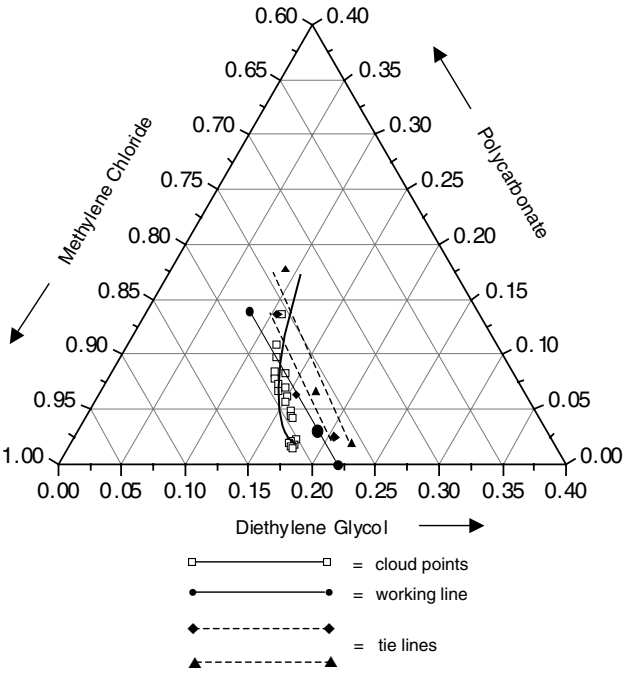

Fig. 3. Phase diagram for PC1/methylene chloride/diethylene glycol at room temperature (20°C).

3.2. Characterization of fractions

For each fraction, MWs, concentrations of modified units I (PSAL) and II (PhSALPhC) and hydroxyl end-groups were determined. Based on NMR and HPLC data there was no evidence for the presence of structure III (Ph-*o*-PhxBz) in our samples. MWs were measured by SEC-UV and SEC-LS. Because of the presence of branched chains, it cannot be assumed without further checking that SEC

Table 1
CPF parameters for PC1 and PC2

	CPF run no.	Feed (w1/w2/w3)[a]	EA (w1/w2)	Working point (w3)	Fractionation temperature (°C), column/condenser	Fluxes (Feed/EA) a: (g/h), b: (ml/min)	Fraction no.: yield (g)
PC1	1	0.780/0.080/0.140	0.780/0.220	0.035	21/8	a: 93/305, b: 1.2/4.0	#1: 77
	2[b]	0.790/0.085/0.125	0.805/0.195	0.032	22/11	a: 85/261, b: 1.1/3.4	#2: 63, #3: 48
PC2	1	0.780/0.080/0.140	0.780/0.220	0.033	21/8	a: 100/321, b: 1.3/4.2	#1: 55
	2[c]	Gel of run #1	0.795/0.205	n.a.	17/10	a: n.a., b: 1.3/4.0	#2: 38, #3: 12[d], #4: 21

[a] w1: methylene chloride, w2: diethylene glycol, w3: polycarbonate.
[b] PC1, CPF run #2 on PC isolated from the gel fraction of CPF run #1.
[c] PC2, CPF run #2 on gel obtained from CPF run #1.
[d] Isolated from column content after CPF run #2.

Table 2
Analytical data for samples PC1 and PC2 and derived fractions

	Sample	SEC-UV			Modified units (ppm)			[OH] (ppm)	Endcap (%)
		M_w (g/mol)	M_n (g/mol)	D	Total	PhSAL	PhSALPhC		
PC1	Total	21,700	9520	2.28	1250	–	1250	570	84
	PC1F1	11,400	6590	1.73	760	–	760	1050	80
	PC1F2	17,700	11,570	1.53	1220	–	1220	675	77
	PC1F3	31,900	24,100	1.32	1870	–	1870	250	82
PC2	Total	23,700	9210	2.57	5260	1795	3465	1185	67
	PC2F1	11,900	6330	1.87	3715	1670	2045	1855	65
	PC2F2	22,100	14,120	1.57	5355	1820	3535	780	68
	PC2F3	28,900	19,090	1.51	5765	1760	4005	610	66
	PC2F4	39,200	24,950	1.57	7045	1855	5190	455	67

delivers true MWs as molecules with different MWs can have the same hydrodynamic volume in diluted solution due to differences in branching density. Since LS detection is less sensitive towards low molecular species, the number average MWs are consistently underestimated by SEC-LS and more reliable M_n values are obtained by SEC-UV. Weight average MWs as determined by both techniques show good agreement. Because of this, SEC-UV MWs are used throughout this paper. Characterization results are summarized in Table 2. The fraction of phenyl carbonate capped end-groups (called endcap%) is calculated from the hydroxyl concentration and number average MW. Fig. 4 shows a SEC-LS overlay plot depicting the MW distributions for the fractions and initial polymer of sample PC2.

The hydroxyl end-group content as well as PhSAL and PhSALPhC structures (I and II) can be conveniently quantified by proton-NMR. Fig. 5 shows the aromatic region of the NMR spectrum of PC2-fraction no. 4 with peak assignments.

The branching concentrations as determined for the fractions are only accurate if fractionation did occur solely by MW and was not significantly affected by branching architecture. Two reasons make us confident this is indeed the case. First, as can be observed from Table 3, the overall branching density of the PC samples investigated is very low. This is highlighted by the calculated ratios of the

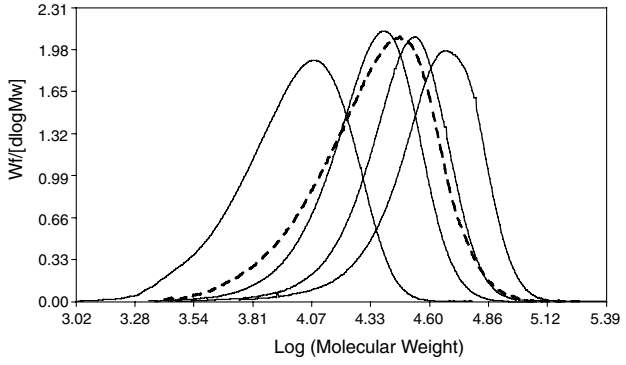

Fig. 4. SEC-LS overlay plot for PC2: initial polymer (dotted line) and derived fractions (solid lines).

mean square radii in solution for branched and linear molecules, $\langle g(m)\rangle_{av}$, which remain very close to 1 except for the highest MW PC2 fraction. The calculated values are based on the Zimm and Stockmayer formula [13] for randomly branched polymers containing trifunctional branching units:

$$\langle g(m)\rangle_{av} = \left[\sqrt{\left(1+\frac{m}{7}\right)} + \frac{4m}{9\pi}\right]^{-1/2} \quad (3)$$

where m is the average number of branching units per molecule. Second, as will become clear from the simulation results, there is an excellent agreement between experimental branching densities of the fractions and the simulation predictions. This implies that the MW measured for the fractions is indeed correct.

Fig. 6 shows how the concentration of PhSAL and PhSALPhC units depend on the fractions number average MW. On the one hand, the concentration of PhSAL structure I units in PC2 is fraction MW independent indicating homogeneous incorporation in the polymer, i.e. the thermal rearrangement reaction leading to PSAL structures is not MW dependent. The endcap level is also constant across the entire MW range, which is an expected result if the BPA units carrying the hydroxyl end-groups are built in statistically. On the other hand, the concentration of PhSALPhC structure II units, i.e. the branching density increases quasi linearly with MW for both polymers. This also means PhSALPhC branching units are not homogeneously distributed across the MW distribution, at first sight a counter-intuitive result, considering that the statistical nature of the polymerization process is confirmed by the results for PhSAL units and end-groups concentrations.

Branching effects can be visualized through Mark–Houwink plots where intrinsic viscosities (SEC-IV) are depicted as a function of MW (determined by SEC-LS). The higher the degree of branching, the lower the intrinsic viscosity will be relative to the absolute MW. For polyethylene for instance, it is known that long chain branched metallocene catalyzed polymers have simple architecture and materials with different branching probabilities are represented in the Mark–Houwink plot by by parallel

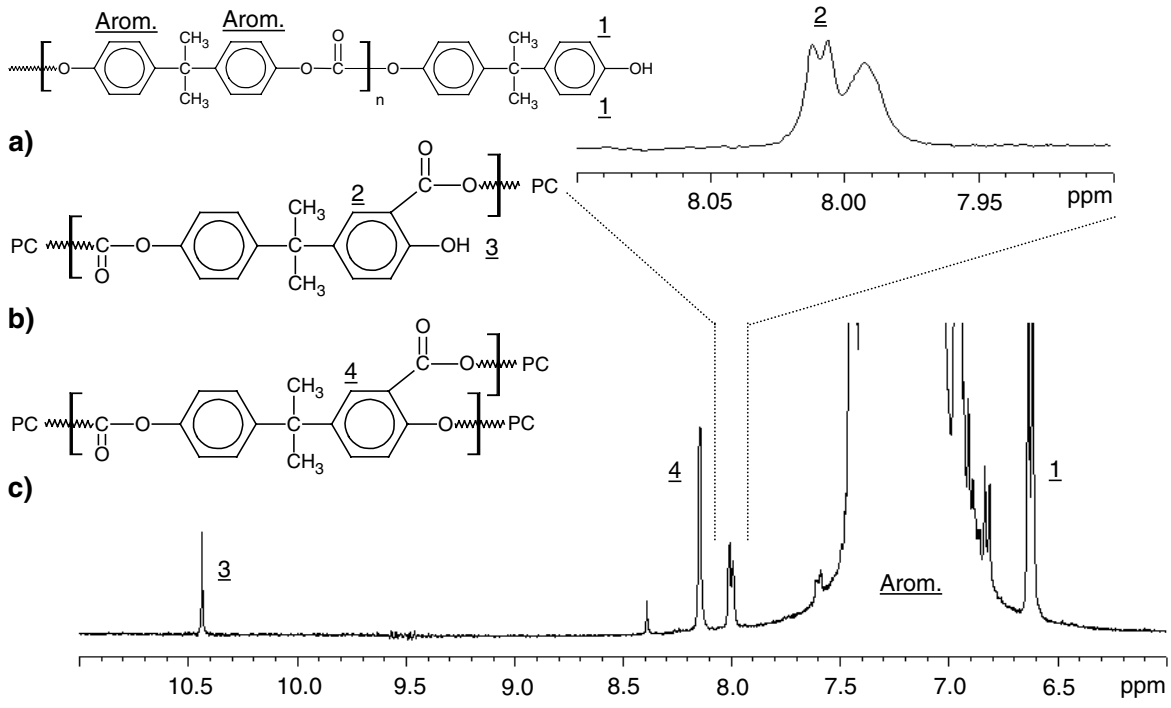

Fig. 5. Aromatic proton-NMR region of PC2, fraction no. 4: (a) BPA-PC; (b) PhSAL, structure I (c) PhSALPhC, structure II.

lines [28]. On the other hand, radical polymerized LDPE polymers have a complex architecture and exhibit a decreasing slope with increasing MW. Fig. 7 shows Mark–Houwink log plots for the initial polymer and the two extreme fractions of PC2. The observed lines are essentially parallel for the lower MW fractions and the whole sample, which is consistent with the overall low degree of branching determined by NMR. For the highest fraction PC2F4, however, there is a slight departure from parallelism. The lower exponent is consistent with the higher degree of branching of this last fraction. For PC1 (not shown), all lines run parallel, reflecting the lower branching density as compared to PC2. On the other hand, the expected relationship between $\langle g(m)\rangle$ and g' (see Table 3) is not observed. Both factors usually relate as $g' = \langle g\rangle^b$, where b has a value between 0.5 and 1.5 depending on the type of branched polymer [12]. Apparently, this empirical formula is not valid for the polymers investigated here. A similar discrepancy for polycarbonate materials was already reported by Bartosiewicz et al. [7].

3.3. Simulations

In order to approach the branching density distribution of the investigated melt-polymerized PC samples from a more theoretical standpoint and to validate experimental results, a simulation model was developed based on a random sampling technique. The MW, end-group and branching

Table 3
Branching data for PC1 and PC2

	Sample	Branching density $\times 10^{-3}$	Average no. of branching units per chain	$\langle g(m)\rangle_{av}$ [a]	SEC-IV g' ($= IV_{br}/IV_{lin}$) (average)
PC1	Total	1.068	0.040	0.996	0.86
	PC1F1	0.650	0.017	0.998	1.04
	PC1F2	1.042	0.048	0.995	0.94
	PC1F3	1.597	0.151	0.984	0.85
PC2	Total	2.955	0.107	0.989	0.82
	PC2F1	1.175	0.044	0.995	0.98
	PC2F2	3.014	0.168	0.983	0.87
	PC2F3	3.413	0.257	0.974	0.80
	PC2F4	4.419	0.434	0.957	0.76

[a] Calculated from Zimm–Stockmayer equation (3).

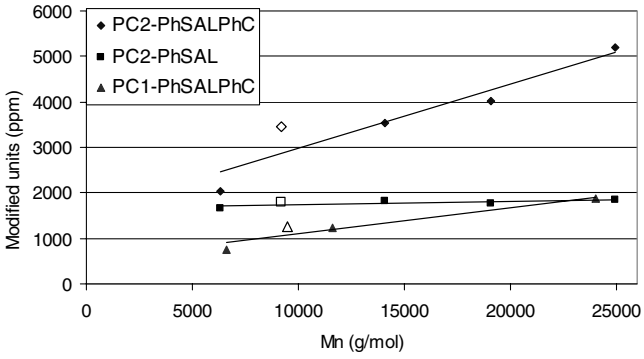

Fig. 6. PhSAL and PhSALPhC concentration as a function of M_n for PC1 and PC2; closed symbols denote the fractions, open symbols the total unfractionated polymer.

data of samples PC1 and PC2 were used as input parameters for the model. The polymers were then 'rebuilt' by a statistical simulation process. Fig. 8 shows the simulated branching density for PC1 fractions as a function of MW. The branching density initially increases with MW and reaches a plateau for very high MWs well beyond the experimental range. The results are qualitatively identical for PC2. Clearly our simulation results for a step-growth polymerization agree qualitatively with Tobita's model [11,12] developed for an addition polymer.

Fig. 9 highlights the agreement between experimental and simulated data by comparing the number of branching units per chain as function of M_n and M_w for PC1 and its fractions. The measured weight average M_ws of the initial polymer and fractions fit very well with the simulation curve while a minor shift is observed for the number average M_w. This latter deviation is most probably caused by the non-randomness of the branching distribution within individual fractions. The branching units are, like the total polymer, not randomly distributed across the MWD of each fraction and chains on the high end of the fraction MWD have proportionally more branching units than chains with shorter M_ws. As a result, the number of branching units per chain is overestimated resulting in the observed shift for the M_n data. Apparently, choosing M_w rather than M_n gives the right 'weighing' to the chains in the various fractions. Very similar results are obtained for PC2 and its fractions. Also here, a minor shift from the simulation curve is observed for M_n data, this shift being only marginally larger than for PC1 due to the higher concentration of branching units in the fractions.

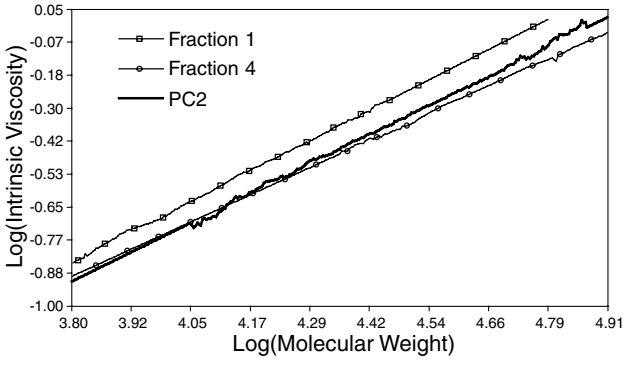

Fig. 7. Mark–Houwink plot for PC2 and derived fraction nos. 1 and 4.

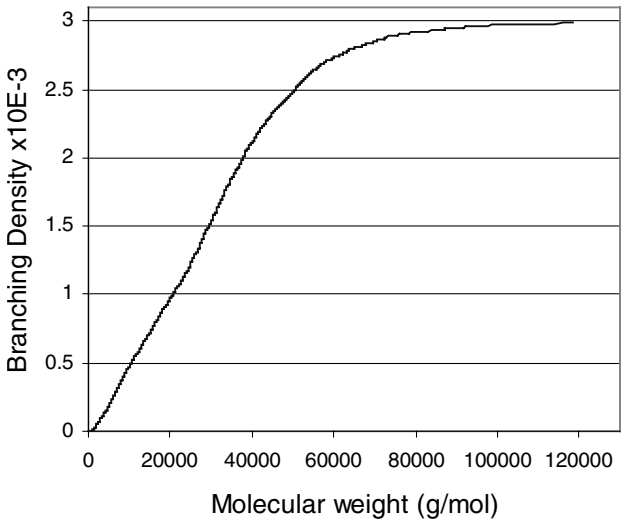

Fig. 8. Simulated branching density distribution for PC1.

4. Conclusions

CPF is an efficient method to fractionate melt-produced polycarbonate materials with low degrees of branching with respect to MW. The technique is capable of delivering preparative (multi-gram) size fractions that can be used for further research. The experimentally determined branching density distributions as derived from the fractions and a random simulation model are in good agreement. The most striking result is the heterogeneous nature of branching density across the MWD. Despite the fact that the result is in agreement with Tobita's findings it must be emphasized that the reaction mechanisms underpinning the two simulations are quite different. Although an increasing branching

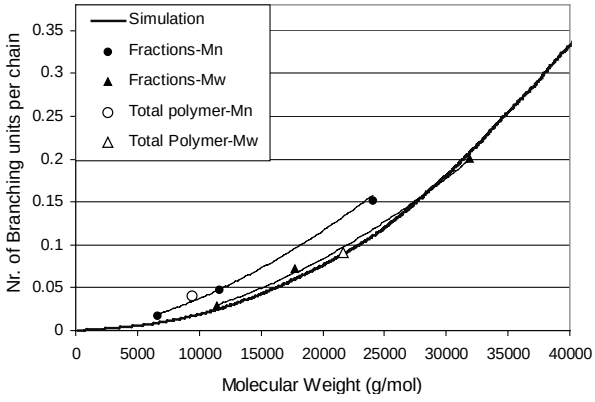

Fig. 9. Experimental and simulated number of branching units per chain as a function of number and weight average MW for PC1.

density with increasing MW seems at first counterintuitive, it simply reflects that under statistical 'thermodynamic' control, branched chains will 'on average' be longer than linear chains, thus concentrating branching points in the high MW fractions. This effect only disappears at very high MW, beyond the experimental reach for PC. On the other hand, PhSAL units and end-groups are distributed homogeneously across the entire MW distribution, as expected.

Acknowledgements

The authors would like to thank Mrs K. Schellenberg for help with the CPF experiments and Prof. J. Devaux for interesting discussions.

References

[1] King Jr. JA. In: LeGrand DG, Bendler JT, editors. Handbook of polycarbonate science and technology, New York: Marcel Dekker, 2000. p. 7 [chapter 2].
[2] Schnell H. Chemistry and physics of polycarbonates, 3. New York: Wiley, 1964. p. 47.
[3] Oba K, Ishida Y, Ito Y, Ohtani H, Tsuge S. Macromolecules 2000;33:8173–83.
[4] Katsuji S. Japanese Patent 9-59371, 1997 (to Teijin Ltd.).
[5] Bailly Ch, Daumerie M, Legras R, Mercier JP. J Polym Sci, Phys Ed 1985;23:493–507.
[6] Marks MJ, Munjal S, Namhata S, Scott DC, Bosscher F, De Letter JA, Klumperman B. J Polym Sci, Polym Chem 2000;38:560–70.
[7] Bartosiewicz RL, Booth C, Marshall A. Eur Polym J 1974;10:783–9.
[8] Cogswell FN. Polymer melt rheology. New York: Wiley, 1981 [chapter 4].
[9] Ward I, Hadley DW. Mechanical properties of solid polymers. Chichester: Wiley, 1993 [chapter 1].
[10] Flory PJ. J Am Chem Soc 1947;69:2893–9.
[11] Tobita H. Macromol Theory Simul 1996;5:129–44.
[12] Tobita H, Hamashima N. J Polym Sci, Polym Phys 2000;38:2009–18.
[13] Zimm BH, Stockmayer WH. J Chem Phys 1949;17:1301–14.
[14] Francuskiewicz F. Polymer fractionation. Berlin: Springer, 1994.
[15] Lunak S, Bohdanecky M. Coll Czech Chem Commun 1965;30:2756–70.
[16] Sitaramaiah G. J Polym Sci, Part A 1965;3:2743–57.
[17] Berry GC, Nomura H, Mayhan KG. J Polym Sci, Part A 1967;2(5):1–21.
[18] Bailly C, Daoust D, Legras R, Mercier JP, Strazielle C, Lapp A. Polymer 1986;27:1410–5.
[19] Glöckner G. Plaste Kautschuk 1965;12:96–102.
[20] Turska E, Dems A, Siniarska M. Bull Acad Polon Sci Ser Sci Chim 1965;13:189–93.
[21] Luo M, Teraoka I. Macromolecules 1996;29:4226–33.
[22] Wolf BA. Adv Mater 1994;6:701–4.
[23] Wolf BA. Makromol Chem, Macromol Symp 1992;61:244–7.
[24] Weinmann K, Wolf BA, Rätzsch MT, Tschersich L. J Appl Polym Sci 1992;45:1265–79.
[25] Weinmann K. PhD Thesis. Germany: University of Mainz; 1992.
[26] Hersh SN, Choi KY. J Appl Polym Sci 1990;41:1033–46.
[27] Kim Y, Choi KY. J Appl Polym Sci 1993;49:747–64.
[28] Metallocene-catalyzed polyethylene. Viscotek universal calibration application note 2. Houston: Viscotek Corporation; 2000.